AD-A055 633 STANFORD UNIV CALIF INST FOR PLASMA RESEARCH F/G 3/2
THE RAPID HEATING OF CORONAL PLASMA DURING SOLAR FLARES: NONEQU--ETC(U)
JAN 78 P R SHAPIRO, J W KNIGHT

UNCLASSIFIED SU-IPR-726 NL

1 OF 1
ADA
055633

END
DATE
FILMED
8 78
DDC

Center for Astrophysics
Preprint Series No. 912

THE RAPID HEATING OF CORONAL PLASMA DURING SOLAR FLARES: NONEQUILIBRIUM IONIZATION DIAGNOSTICS AND REVERSE CURRENTS

Paul R. Shapiro*
Harvard-Smithsonian Center for Astrophysics
and
J. W. Knight
Institute for Plasma Research and Department of Applied Physics
Stanford University

*John Parker Fellow, 1977-78

ABSTRACT

A simple method is presented for diagnosing the electron temperature and density of a rapidly heated, coronal-type plasma from observable, non-equilibrium enhancements of X-ray line emission. This method, it is argued, is applicable to the study of solar flares. Accordingly, theoretically predicted line enhancements are given for a representative selection of X-ray lines prominent in the preflare coronal emission spectrum. Some of these predicted line enhancements should soon be observable with instruments aboard the Solar Maximum Mission.

Mechanisms, involving energetic electron beams and reverse currents, for the heating of coronal flare plasma rapidly enough to produce these non-equilibrium effects are examined. A time-dependent calculation of Joule heating by the reverse current is presented for two illustrative electron beam strengths. For the first, classical Coulomb resistivity is assumed for the ambient plasma, while for the second, anomalous resistivity is assumed to result from the onset of electrostatic ion-cyclotron turbulence. The results suggest that rapid heating can occur by a variety of mechanisms.

Subject headings: plasmas--Sun:corona--Sun:flares--Sun:X-rays

I. INTRODUCTION

Observational and theoretical evidence suggests that hard X-ray emission (10-100 keV) during solar flares may be accompanied by extremely rapid heating of coronal plasma. Temporal fine structure on time scales at least as short as a second have been reported for the hard X-ray bursts (for instance, Van Beek et al. 1974; Beigman et al. 1971; Kane and Anderson 1970; Frost 1969). If this hard X-ray emission is thermal electron-ion bremsstrahlung (as suggested by Chubb et al. 1966, for instance) then very hot plasma ($kT_e \gtrsim 50$ keV) must be created in a very short time. Alternatively, the hard X-rays can be interpreted as non-thermal electron-ion bremsstrahlung resulting from the streaming of energetic non-Maxwellian electrons from the corona to the chromosphere (for instance, Kane and Anderson 1970). This electron stream is a current which, if unneutralized, implies a self-magnetic-field with an energy orders of magnitude greater than the total observed flare energy (Colgate et al. 1976, Hoyng et al. 1976). It is well known, however, that when such an electron stream is introduced in a plasma, a reverse current develops that balances or nearly balances the beam current (Cox and Bennet 1970; Hammer and Rostoker 1970). The existence of this reverse current has a variety of implications for the ambient coronal plasma (Knight and Sturrock 1977; Brown and Melrose 1977; Spicer 1977). Among these is extremely rapid heating.

If the temperature of coronal electrons increases during flare hard X-ray bursts on a time scale which is shorter than the characteristic ionization times of plasma ions, a lack of equilibrium between ionization and recombination results which can dramatically affect the emergent X-ray spectrum (Shapiro and Moore 1977). The effect of non-equilibrium ionization of coronal

flare plasma on selected X-ray line intensities has been illustrated by Kafatos and Tucker (1972) and Mewe and Schrijver (1975). Recently, the effect on the complete line and continuum spectrum from 1 to 250 Å has been calculated in detail for a model in which a magnetic loop of preflare coronal plasma initially in ionization equilibrium at a typical quiet coronal temperature ($\sim 2 \times 10^6$ K) and at a density of between 10^{10} and 10^{11} cm^{-3} is heated within a fraction of a second to a temperature close to 10^8 K (Shapiro and Moore 1977). Among the non-equilibrium effects found for this model was a burst-like enhancement of the soft X-ray flux from the loop. It was argued there that such effects are likely to be common to a fairly general class of scenarios involving rapid coronal heating.

The magnitude of such soft X-ray enhancements as a function of wavelength should reflect the particular temperature to which the plasma electrons are heated, while the decay time for the enhancements should depend upon both the temperature and the density after heating as reflected in the ionization times of the line-emitters. This suggests that observations of such non-equilibrium ionization effects may provide a useful diagnostic of the temperature and density of rapidly heated coronal flare plasma. Since the reverse current mentioned above may imply rapid heating, such effects may provide observational confirmation of theoretical reverse current models, or at least place constraints on them.

Our purpose in § II will be to show how such non-equilibrium spectral behavior can be used as simply as possible to determine the temperature and density of impulsively heated flare plasma. In § III we briefly describe the ways in which electron beam and reverse current models involve rapid heating. We then present the results of an illustrative, time-dependent calculation of this heating for the case of Joule heating by the reverse current. We

consider two electron beam strengths in this calculation, one for which it is reasonable to assume classical Coulomb resistivity for the ambient plasma and one for which an anomalous resistivity is assumed to result from the onset of electrostatic ion-cyclotron turbulence. We summarize our discussion in § IV.

II. THE DIAGNOSTICS

We shall assume, for the sake of simplicity, that the coronal plasma under discussion has a uniform electron temperature T and density n_e. Implicit in this is the assumption that the electrons can Maxwellianize faster than the time scales for any of the other processes considered here which require a well-defined T. For the higher temperatures and lower densities among those which we consider, this may not be possible by classical Coulomb collisions among plasma electrons, alone. In some cases, for instance, not only is this Maxwellianization time too long, but the electron-electron Coulomb mean-free-path is longer than the characteristic spatial extent of the coronal plasma. In these cases, we need simply interpret T as representative of the mean energy to which the electrons are heated. We shall say more about this later. The possibility that rapid heating of coronal plasma will also cause a pressure imbalance and subsequent mass motion is ignored here. This is based upon the fact that the appropriate hydrodynamical time scale is usually longer than the ionization and excitation time scales considered here. More generally, we ignore the possibility that the electron temperature after heating evolves on a time scale as short as those of these atomic processes by <u>any</u> means, including thermal conduction. Lastly, we make the very reasonable assumption that the plasma is in ionization equilibrium prior to rapid heating.

The rate for collisional excitation of the i to j transition of a positive ion by Maxwellian electrons of temperature T and number density n_e, where i is the ground level and j is the upper level, can be written as

$$n_e C_{ij} = 1.70 \times 10^{-3} n_e E_{ij}^{-1} f_{ij} \bar{g}(E_{ij}/kT) T^{-\frac{1}{2}} \exp(-E_{ij}/kT) \text{ s}, \qquad (1)$$

where E_{ij} is the energy difference (in eV) between the ground level and level j, k is the Boltzmann factor, f_{ij} is the absorption oscillator strength, and $\bar{g}$ is the integrated effective Gaunt factor (Van Regemorter 1962). We shall be particularly interested here in situations in which E_{ij}/kT is a small number. In that case, the Bethe approximation is valid and we can replace $\bar{g}$ by the asymptotic form of the actual integrated Gaunt factor for high electron energies. If we define $y \equiv E_{ij}/kT$, then this gives (for $y \leq 0.01$)

$$g(y) \approx (\sqrt{3}/2\pi)(-0.57722 - \ln y). \qquad (2)$$

(cf. Van Regemorter 1962). For low electron energies ($y \geq 1$), on the other hand, at least in the case of the optically allowed transitions in which we are primarily interested, $\bar{g}$ can be taken as constant and roughly equal to 0.2 (Van Regemorter 1962).

The line emission rate for spontaneous radiative decay of the upper level j into a level k subsequent to the collisional excitation described by equation (1) is given by

$$\Lambda_{jk} = n_e n_H A(Z) y_{Z,z} E_{jk} C_{ij} B_{jk} \text{ eV cm}^{-3} \text{ s}^{-1}, \qquad (3)$$

where n_H is the hydrogen number density, A(Z) is the abundance of element Z relative to hydrogen, $y_{Z,z}$ is the fraction of atoms of atomic number Z which are in the zth ionic stage, and B_{jk} is the branching ratio indicating the fraction of decays of level j which end in level k. This ignores the typically minor contributions to the line emission rates considered here from such

things as cascades from upper levels, dielectronic recombination, and the collisional depopulation of nearby mestastable levels. The temperature dependence of this line emission rate is then contained entirely in the product $y_{Z,z}\,\bar{g}(y)T^{-\frac{1}{2}}\,e^{-y}$. What happens to the rate if T is instantaneously increased by a factor α?

Since $y_{Z,z}$ is a quantity which varies on a time scale comparable to the ionization time for that species, any increase in T which occurs faster than this will leave $y_{Z,z}$ unaffected. Accordingly, if we define β as the factor of change in the line emission rate resulting from the factor α increase in T, then

$$\beta = (\bar{g}(y/\alpha)/\bar{g}(y))\,\alpha^{-\frac{1}{2}}\,e^{-y(1/\alpha-1)}. \qquad (4)$$

For small values of y/α, where $y \geq 1$, we can use equation (2) for $\bar{g}(y/\alpha)$ and replace $\bar{g}(y)$ by 0.2. In that case,

$$\beta \simeq 1.38(-0.577 - \ln y + \ln\alpha)\,\alpha^{-\frac{1}{2}}\,e^{-y(1/\alpha-1)}. \qquad (5)$$

As an example, let y=1. Then for α=10, β=1.8, and for α=100, β=1.5. As we shall see when we consider selected lines, β can sometimes be quite large. For a given y, β has a maximum as a function of α given by $\beta_{max} = \beta(\alpha_{max})$, where

$$\alpha_{max} \simeq 17y. \qquad (6)$$

When y=5.88, for example, α_{max}=100, and the corresponding β_{max}=105!

Equation (5) suggests a simple temperature diagnostic for the rapidly heated coronal plasma: For a given initial, pre-flare (i.e. prior-to-heating), coronal temperature, an X-ray line can be chosen which is fairly prominent in the spectrum of the ionization equilibrium at that T (using a tabulation such as that of Kato, 1976). A measurement of β at the time of heating then permits the use of equation (5) to solve for α and, hence, the post-heating temperature, αT.

This X-ray line should be chosen so as to maximize the information content of the diagnostic measurement. For a given y, for instance, a temperature increase by a factor α_{max} will give the largest line strength enhancement. The larger y is (i.e. the larger the energy required to excite the line is), moreover, the larger β is for a given α. The larger β is, the greater is the significance of the measurement. For a given initial T, however, there is an upper limit to the magnitude of the y's which belong to those lines which can be called "prominent." Moreover, for a given α, a post-heating increase in the level of the thermal bremsstrahlung (TB) continuum at the wavelength of a particular line may accompany the increase in line strength and may be large enough to make even the enhanced line difficult to observe, depending upon instrumental wavelength resolution.

In view of these considerations, the best and most general approach seems to be the judicious choice of a selection of the strongest lines emitted by the ionization equilibrium plasma at the initial T, a selection which covers a range of wavelengths and a range of y's. At the very least, two lines with different y's must be considered since the existence of a maximum in β as a function of α implies that, in some neighborhood of α_{max}, α is a double-valued function of β. In any case, increasing the number of lines observed increases the significance of this measurement of α.

We present in Table 1 a representative selection of thirteen lines suitable for measuring α as described above, for the case in which the initial electron temperature before heating is 3×10^6 K, a value typical of the corona above an active region (Noyes 1971). We have limited our selection to optically allowed transitions, for which the density-dependent effects described, for instance, by Mewe and Schrijver (1975) do not occur. Table 1 gives the enhancement factor β for these lines for a variety of temperature

increases. Results range from an enhancement factor of 133 for the Mg XI line at 7.85 Å for α=100 to a factor less than one for the Fe XVI line at 76.60 Å for α=1000. The ease with which these enhancement factors can be measured depends on a variety of things including the duration of the enhancements relative to instrumental time resolution, instrumental wavelength resolution and the confusion caused by nearby lines, and the strength of the line relative to the continuum. Inasmuch as this continuum may, itself, provide another temperature diagnostic, as well, we briefly consider it further.

For simplicity, we consider electron-ion thermal bremsstrahlung only and ignore the contribution to the continuum from radiative recombination and the two-photon process. We note, however, that in the case considered by Shapiro and Moore (1977), the two-photon process was as important as TB for the wavelength range from 18 to 100 Å. The TB emissivity can be written as

$$j_\nu = 6.8 \times 10^{-38} \sum_Z z^2 n_e A(Z) n_H y_{Z,z} T^{-\frac{1}{2}} \bar{g}_{ff}(\nu,T) e^{-h\nu/kT} \quad \text{erg cm}^{-3}\,\text{s}^{-1}\,\text{Hz}^{-1} \tag{6}$$

(Tucker 1975), where the summation is over all ions in the plasma (the greatest contribution coming from H and He) and $\bar{g}_{ff}$ is the temperature-averaged Gaunt factor summarized by Tucker (1975) (for the cases of interest here) as follows:

$$\bar{g}_{ff}(\nu,T) \cong (\sqrt{3}/\pi)\ln(2.2kT/h\nu) \quad \text{for } h\nu/kT \ll 1, \tag{7a}$$

$$\cong 1 \quad \text{for } h\nu/kT \cong 1, \tag{7b}$$

$$\cong (kT/h\nu)^{0.4} \quad \text{for } h\nu/kT > 1. \tag{7c}$$

In order to define an enhancement factor for the TB continuum, as well as make comparisons of the continuum level with line strengths, equation (6) must be

integrated over some frequency range. As expressions for this integrated quantity which take proper account of the frequency dependence of $\bar{g}_{ff}(\nu,T)$ do not, to the best of our knowledge, already exist in the literature, we give our version of them in what follows.

For a fully ionized cosmic plasma, the summation $\sum n_e A(Z) n_H y_{Z,z} z^2$ may be approximated by $1.4n_e^2$, according to Tucker (1975). In that case, let ε_1 and ε_2 be the lower and upper limits on the photon energy range under consideration, respectively, and let $u_{1,2}=\varepsilon_{1,2}/kT$. The energy emitted in the photon energy band between ε_1 and ε_2, $P_B(\varepsilon_1,\varepsilon_2,T)$, can then be written as:

$$P_B(\varepsilon_1,\varepsilon_2,T) \equiv \int_{\varepsilon_1/h}^{\varepsilon_2/h} j_\nu \, d\nu \quad \text{erg cm}^{-3}\,\text{s}^{-1}$$

$$= 1.98 \times 10^{-27} n_e^2 T^{\frac{1}{2}} f(u_1,u_2). \tag{8}$$

The three cases represented in equation (7) then, it can be shown, give the following:

$$f(u_1,u_2) \cong 0.55(0.788(e^{-u_1} - e^{-u_2}) - (1-e^{-u_2})\ln u_2 + (1-e^{-u_1})\ln u_1 + (u_2 - u_1) - 0.25(u_2^2 - u_1^2) + 0.056(u_2^3 - u_1^3)) \quad \text{for } u_{1,2} < 1, \tag{9a}$$

$$f(u_1,u_2) \cong (e^{-u_1} - e^{-u_2}) \quad \text{for } u_{1,2} \cong 1, \tag{9b}$$

$$f(u_1,u_2) \approx u_1^{-0.4}(0.48(e^{-u_1} - e^{-u_2}) + 0.64u_1(E_1(u_1) - E_1(u_2)) - 0.12u_1^2((e^{-u_1}/u_1 - e^{-u_2}/u_2) - E_1(u_1)+E_1(u_2))) \quad \text{for } u_{1,2} > 1, \tag{9c}$$

where $E_1(u)$ in equation (9c) is the standard exponential integral and where, for $u > 1$, one can use

$$E_1(u) \approx u^{-1}e^{-u}\frac{u^2 + 2.33u + 0.25}{u^2 + 3.33u + 1.68} \tag{9d}$$

The TB enhancement factor β_{TB} is a function of the energy window in which an observation is to be made and can be written as

$$\beta_{TB} \equiv \frac{P_B(\varepsilon_1/\alpha,\ \varepsilon_2/\alpha,\ \alpha T)}{P_B(\varepsilon_1,\ \varepsilon_2,\ T)} = \alpha^{\frac{1}{2}}\frac{f(u_1/\alpha,\ u_2/\alpha)}{f(u_1,\ u_2)} \tag{10}$$

This ratio involves different pairs of the expressions given in equation (9) depending upon the particular values of ε_1/kT, ε_2/kT, and α. In principle, equations (9) and (10), together with a measurement of β_{TB}, provide another means of solving for α. In any case, equations (3) and (9) determine, for a given observational energy band, the strength of a line in that band relative to the TB continuum. The question of whether a particular line enhancement, is observable above the TB continuum, as well as that of whether the TB enhancement, itself, can be independently measured, can be answered only when one knows the wavelength resolution and sensitivity of the observing instrument.

The time scales on which the non-equilibrium-enhanced X-ray lines decay are just the ionization times of the species responsible for the lines; the lines disappear when the ionic stages which produce them are

ionized away. This suggests an electron density diagnostic for the rapidly heated coronal plasma as follows: <u>The ionization time is a function of both T and n_e. Once T is determined by the prescription given above, however, the ionization times determined from the line emission decay times are just inversely proportional to the electron density</u>.

The thermal electron collisional ionization time for an ion of nuclear charge Z in the corona is given by Lotz (1968, 1969) as

$$\tau_I = 1.39\times10^4\, n_e^{-1}T^{\frac{1}{2}}\left(\sum_{\xi}^{-1}a^{-1}I_{Z,z}(E_1(y_I)-be^c\frac{y_I}{c+y_I}E_1(c+y_I))\right)^{-1}, \tag{11}$$

where $y_I = I_{Z,z}/kT$, $I_{Z,z}$ is the ionization potential in eV of one shell of the z^{th} stage of element Z, and a, b, c, and ξ are tabulated constants (where, in general, $a \approx 5$, $0 \le b \le 1$, $0 \le c \le 1$, and $1 \le \xi \le 10$), and where the summation is over all contributing n, l subshells. When y_I is small, we can ignore the second term inside the innermost parentheses in equation (11) and replace $E_1(y_I)$ by $(-0.577 - \ln y_I + y_I)$.

Table 2 shows the collisional ionization times and, hence, the expected line-enhancement decay times for the ions included in Table 1 for the same selected temperature increases, using equation (11). These times are normalized to the case of $n_e = 10^9 cm^{-3}$, a typical value for the corona above an active region (Noyes 1971). As mentioned earlier, the fact that Maxwellianization may not, in some cases, be rapid enough to justify the assumption of a well-defined electron temperature can be accommodated by interpreting αkT as a characteristic mean energy of the heated electrons. For instance, the ionization times given by equation (11) and shown in Table 2 are simply uniformly 20% higher than would be calculated for a monoenergetic distribution of electrons of energy E_o

roughly equal to $\frac{1}{2}\alpha kT$. It should be noted that autoionization is important for a few of the ions and, in a more accurate treatment, this would slightly reduce the time scales shown in Table 2 for these ions. Inasmuch as τ_I is just inversely proportional to n_e, measurement of the decay times of the line enhancements is much more sensitive a diagnostic of n_e than the measurement discussed earlier was of T.

In concluding this section, we mention another more commonly known temperature diagnostic which, while not based upon a non-equilibrium effect, takes a particularly simple form in the case discussed here. Using equations (1), (2), and (3), and the fact that y/kT is small for the lines considered, it can be shown that the ratio of line intensities of a pair of lines produced by the same ion gives the electron temperature T after heating according to the equation

$$T = \exp\left((3.71 \ln E_2)R - (3.71 \ln E_1)C)/(R - C) \right), \quad (12)$$

where

$$C = (f_1 B_1 E_1)/(f_2 B_2 E_2),$$

and where $f_{1,2}$, $B_{1,2}$, and $E_{1,2}$ are the oscillator strengths, branching ratios, and excitation energies, respectively, of the lines and R is the measured ratio of line 1 to line 2. This diagnostic has the particular virtue of allowing the "monitoring" of the electron temperature both during and after the rapid heating, in the event that either the heating is not much faster than characteristic ionization times or the temperature continues to change rapidly even after the heating takes place.

We have not considered here line emission by ionic species which become abundant in the coronal plasma only after the non-equilibrium ionization has had a chance to populate their ionic stage. We have been

careful, in fact, to avoid discussing any such non-equilibrium effects which can be calculated only by performing a detailed, model-dependent, numerical integration of ionization rate equations such as done by Shapiro and Moore (1977). We have, as a result, also avoided discussing over-all effects on the X-ray spectrum, such as the soft X-ray burst found by Shapiro and Moore in certain broad energy bands. This, too, was for the purpose of showing that diagnostics could be found which did not require a massive computer calculation of detailed spectra. In the end, of course, one will have to turn to the more detailed models to refine the highly simplified and idealized picture on which this work has been based.

III. ELECTRON BEAMS, REVERSE CURRENTS, AND RAPID HEATING

A number of authors have recently considered the origin and consequences of reverse currents in solar flares (for instance, Knight and Sturrock 1977; Brown and Melrose 1977; Spicer 1977). Hoyng et al. (1978) have summarized some of these considerations as they relate to diagnostics of hard X-ray emission in solar flares in general. We shall briefly describe how the electron beams and reverse currents can result in rapid coronal heating.

Let us assume that the electron beam exists. The ambient plasma then responds to the beam by neutralizing the beam current with a reverse current of thermal electrons. This neutralization condition implies a reverse current drift velocity for the background thermal electrons given by $v_d = cj/n_e e$, where j is the beam current density. There are then two potentially important sources of energy exchange between the streaming, energetic electrons and the ambient plasma electrons. The first is just the energy loss suffered by beam electrons directly in Coulomb collisions

with ambient electrons, a loss which, for a given beam-electron energy distribution, is just proportional to $n_e j$. The second is the Joule heating of the ambient plasma which results from the finite resistivity η encountered by the reverse current in the plasma, a loss proportional to ηj^2. The ratio of the reverse current Ohmic losses to the beam Coulomb losses is, therefore, just proportional to the drift velocity v_d. There are two cases which can accordingly be distinguished for a given j.

In one case, the density of the ambient plasma is high enough that at least the lower-energy electrons in the beam can lose their energy by Coulomb collisions with the ambient electrons before they can stream out of the corona. In this case, the drift velocity of background plasma thermal electrons required to neutralize the beam current may be quite low, making the ratio of reverse current Ohmic losses to direct Coulomb losses low, as well. Nevertheless, the Coulomb exchange with beam electrons is, by itself, sufficient to produce rapid heating of the ambient electrons. This is the situation considered by Shapiro and Moore (1977).

Alternatively, the density of the plasma through which the energetic electrons stream may be low enough to make the Coulomb collision mean-free-path larger than the characteristic spatial extent of the plasma. In this case, v_d is higher than in the first case and the direct Coulomb exchange is unimportant, but the reverse current Joule heating alone can rapidly heat the ambient plasma.

The rate at which the background plasma is heated by the reverse current depends on the beam current density and the ambient plasma density and temperature. If the ratio of v_d to the electron thermal velocity ($v_{t,e} = (2kT/m_e)^{\frac{1}{2}}$) is large enough, the background plasma may be unstable to the growth of electrostatic plasma turbulence which can dramatically

enhance the plasma resistivity and, therefore, the reverse current heating rate. For example, the reverse current will be unstable against the excitation of ion-acoustic or electrostatic ion-cyclotron turbulence unless, for T_e and T_i the electron and ion temperatures, respectively, (Kindel and Kennel 1971)

$$v_d/v_{t,e} \lesssim \begin{cases} 2.5 & \text{for } T_e \simeq .1\ T_i \text{ (ion-acoustic turbulence)} \\ .9 & \text{for } T_e \simeq .3\ T_i \text{ (ion-cyclotron turbulence)} \\ .3 & \text{for } T_e \simeq T_i \text{ (ion-cyclotron turbulence)} \\ .1 & \text{for } T_e \simeq 3\ T_i \text{ (ion-cyclotron turbulence)} \\ .05 & \text{for } T_e \simeq 10\ T_i \text{ (ion-acoustic turbulence)} \end{cases} \quad (13)$$

Reverse current heating is a self quenching process. If the reverse current is stable against the growth of electrostatic turbulence, then, as the plasma is heated by the reverse current, the resistivity decreases and the reverse current losses are reduced. If the reverse current is unstable to the growth of electrostatic turbulence, the plasma will be heated until the instability criterion is no longer satisfied. It is of interest to estimate the magnitude of the heating due to the reverse current to determine under what circumstances it may produce observable effects of the kind discussed in §II.

Knight and Sturrock (1977) analyzed an idealized, one-dimensional, steady-state model of an electron beam decelerated by the reverse current electric field in a magnetic flux tube of constant cross section. They neglected Coulomb collisions between the beam electrons and the ambient plasma, as well as the dynamics of the plasma, but a straightforward extension of their analysis should suffice to provide estimates of the importance of reverse current heating. Since we expect reverse currents to be established on time scales ($2\pi/\omega_{p,e} \lesssim 10^{-8}$ s) much shorter than the time scale for heating of the plasma ($\gtrsim 10^{-2}$s), it should be a reasonable approximation to use the steady-state results of Knight and Sturrock for the velocity distribution of the beam

electrons. They adopted a velocity distribution for the injected energetic electrons of the form

$$f(v) = \frac{K}{(v_o^2 + v^2)^\gamma} \tag{14}$$

This is a power law at high energies which flattens at low energy, the "knee" being characteristc by v_o. Since many impulsive hard X-ray bursts have nearly power law spectra (Kane and Anderson 1970, Datlowe 1975) and since the emergent bremsstrahlung spectrum depends on the energy spectrum of the injected electrons and to some extent the structure of the atmosphere the stream encounters (Davis et al. 1977), this simple form should provide an adequate basis for the present calculation. Knight and Sturrock found the current density (emu) carried by this primary electron stream as a function of a resistivity weighted measure of the distance, s, from the injection point of the beam to be

$$j(s) = \frac{K}{2(\gamma-1)c}\left(v_o^{2\gamma} + \frac{\gamma}{\gamma-1}\frac{e^2K}{m_e c}\xi\right)^{-((\gamma-1)/\gamma)} \tag{15}$$

where ξ is defined by the relation

$$d\xi = \eta ds \tag{16}$$

and the boundary condition $s = \xi = 0$ at the injection point. The condition that a reverse current be induced in the background plasma to neutralize this primary electron stream is then satisfied simply by equating the reverse current density with this beam current density.

We have calculated the heating due to reverse currents for two injected energetic electron fluxes. The heating rate was taken to be just that which results from the Ohmic losses suffered by the reverse current and is given by

$$\frac{\partial T}{\partial t} = \frac{1}{3n_e}\eta j^2 \tag{17}$$

The electron and ion temperatures were assumed to be equal. We shall say more about this assumption later. At each time step the current at each spatial grid point was calculated using equation (15). The time step was regulated so that the largest change in temperature at any grid point was 1% in one time step. The atmosphere was assumed static; that is, the number density was held constant in time. We adopted v_o corresponding to 25 kev and a power law index, $\gamma = 2.5$ for the energetic electron beam. The results for an injected energetic electron number flux ($v \geq v_o$) of 1.414×10^{17} cm^{-2} s^{-1} are displayed in Figure 1 while similar curves for an injected flux of 5.656×10^{17} are displayed in Figure 2. Figure 3 depicts the density structure of the model atmosphere. The abscissa, I, of the figures is integrated number density from the injection point, defined by

$$I(s) = \int_0^s n(s')ds' \tag{18}$$

where n is the total number density (sum of neutral hydrogen and proton density). Figure 1 shows the temperature as a function of I for two times, 1 s and 5 s after the injection of the beam. Figure 2 displays temperature after .25 s and 1 s. Thermal conductivity was neglected in these calculations, but computer runs with thermal conductivity included indicated that thermal conductivity did not have significant effects for the short time scales ($\lesssim$ 5 s) involved in this calculation.

The electrical resistivity used in the calculations depended on the reverse current drift velocity as indicated below:

$$\eta = \begin{cases} \eta_s & v_d \leq 13 v_{t,i} \\ \eta_s + \eta_A & v_d \geq 13 v_{t,i} \end{cases} \tag{19}$$

where $v_{t,i} = (2kT_i/m_p)^{1/2}$ for T_i the ion temperature, m_p is the proton mass, η_s is the resistivity due to Coulomb collisions derived by Spitzer (1962), and η_A is an anomalous resistivity due to the presence of electrostatic ion-cyclotron turbulence calculated by Ionson (1976). For the smaller energetic electron flux, the reverse current drift velocity did not exceed the critical velocity for the onset of electrostatic ion-cyclotron turbulence. In this case the temperature of the tenuous coronal plasma was raised by about a factor of 2, but most of the beam energy was deposited in the dense portion of the model atmosphere.

The larger electron flux, however, caused the reverse current drift velocity to exceed the critical velocity in the low density portion of the atmosphere, resulting in an anomalous resistivity and an order of magnitude increase in the temperature in these regions in a relatively short time. This is precisely the kind of rapid heating which would result in the non-equilibrium soft X-ray enhancements discussed in §II. We would predict, in this case, that the line enhancements given in Table 1 for $\alpha = 10$ occur, with decay times given in Table 2 for $\alpha = 10$.

Since Coulomb collisions were neglected in this calculation, the heating of the denser portion of the atmosphere is not calculated accurately after the first few tenths of a second. If collisions were taken into account for the primary electrons in the beam, the heating of the denser regions below the corona would be more localized and higher temperatures would be reached. However, the results presented here indicate that an energetic electron beam may significantly heat the low density coronal plasma much more rapidly than by direct Coulomb collisions.

The time for electron and ion temperatures to equilibrate by Coulomb collisions assuming only one species rather than both species are heated

as we have assumed may be estimated from (Spitzer 1962) as

$$t \sim 12.6\, n^{-1}(T_e + \frac{m_e}{m_i} T_i)^{3/2} \text{ s.} \qquad (20)$$

For the temperatures, densities, and time scales considered here, Coulomb collisions alone will not establish equal electron and ion temperatures. We have taken $T_e = T_i$ for computational convenience, however, and must, therefore, address the question of whether one species is preferentially heated.

For the case depicted in Figure 1, for which the resistivity is just classical Spitzer resistivity, only the electrons are heated at first. According to equation (20), the ions are not likely to be heated significantly in turn by energy exchange with the electrons. The heat capacity of the plasma is therefore reduced by a factor of 2, and the times given in Figure 1 should simply be reduced by a factor of 2.

The situation in which plasma turbulence develops, as for the case depicted in Figure 2, is considerably more complicated. As we have indicated, the critical drift velocity for the onset of electrostatic ion acoustic or ion-cyclotron turbulence depends on the ratio T_e/T_i. Just what happens when this drift velocity is exceeded is not well understood, however,

The anomalous resistivity which we have assumed to result from the presence of electrostatic ion-cyclotron turbulence was calculated by Ionson (1976) under the assumptions that the turbulence saturates by ion resonance broadening (Dum and Dupree 1970) and $T_e = T_i$. Palmadesso *et al.* (1974), on the other hand, made the first of the assumptions but calculated the heating rates of the electrons and ions. They find that the ions are heated much more substantially than the electrons, and Papadopoulos (1977) has subsequently concluded that the instability turns off when the ion heating has proceeded to the point at which the instability criterion is no longer satisfied.

If only the ions are heated, the situation will differ from that which we have depicted in two ways. First, the temperature plotted in Figure 2 should be interpreted as T_i, not T_e, and the times given reduced by a factor of two for the same reason those in Figure 1 should be reduced if only the electrons get heated. Second, and more important, the line enhancements predicted here are based on the assumption that T_e, in particular, increases. These enhancements would not be expected if only the ions were to be heated. We note, however, that the experimental evidence for ion heating (e.g. Kelly et al. 1975) is not conclusive, and anomalous electron heating has also been observed in the presence of ion-cyclotron turbulence (e.g. Correll et al. 1975).

It has also been suggested that the ion-cyclotron turbulence saturates, not by ion resonance broadening, but by the formation of a plateau on the electron velocity distribution, instead, in which case no significant anomalous resistivity results (Papadopoulos 1977). If this happens, then as in the case without plasma turbulence, only the electrons are heated at first, at a rate given approximately by classical resistivity. In this case, however, larger electron beam current densities must have been involved to begin with in order for the reverse current drift velocity to have exceeded the critical velocity for the onset of ion-cyclotron turbulence. Since j is larger than in the case without turbulence, the classical heating rate ($\propto j^2$) is, itself, higher for this case. If the electrons are heated sufficiently this way, the critical drift velocity for the onset of ion-acoustic turbulence will be exceeded. In that case, the electrons will be heated until the criterion for instability is no longer satisfied, or, namely, until

$$v_d \approx c_s \approx (kT_e/m_i)^{\frac{1}{2}}, \qquad (21)$$

where c_s is the sound speed.

This latter scenario for rapid electron heating would apply, for instance, to an electron beam strength equal to that assumed in Figure 2. More precisely, assuming the ion-cyclotron turbulence does saturate by electron plateau formation, a beam of this strength would result first in electron heating given approximately by the Figure 1 results with a time scale reduced by a factor of four. After roughly one second, ion-acoustic turbulence would develop, resulting in explosive heating of the electrons to a final temperature which can be estimated from

$$T_e \approx m_i v_d^2/k \approx 10^{10}\ \text{K}, \qquad (22)$$

which corresponds to $\alpha \approx 3000$.

In short, the exact behavior of the ratio T_e/T_i is not well understood and cannot be determined without a much more detailed analysis than would be appropriate for a paper of this scope. We have assumed $T_e \approx T_i$ as a useful and reasonable approximation with which to estimate the magnitude of the reverse current heating. As discussed above, however, temperature enhancements, α, even larger than the largest values shown in Tables 1 and 2 are quite possible.

IV. CONCLUSION

We have examined the possibility that during solar flares, the electron temperature of coronal plasma is significantly increased in a time which is smaller than the characteristic ionization times of the plasma ions. In this event, the one-to-one correspondence between T_e and the emergent X-ray spectrum which can otherwise be assumed for a homogeneous plasma in a steady-state ionization equilibrium ceases to exist. We have presented a simple method for diagnosing the electron temperature and density of such a heated,

coronal plasma based upon non-equilibrium line-emission strength enhancements which are expected to occur for lines present in the plasma spectrum just prior to rapid heating. The magnitude of these enhancements, it is shown, can be used to determine T_e, while their decay times subsequently yield n_e.

We have discussed mechanisms which involve electron beams and reverse currents by which the coronal plasma may be rapidly heated during solar flares. We have, moreover, calculated the reverse current heating which results from two illustrative beam strengths. For the smaller beam current density, the resistivity is classical and the heating, while rapid, is too small to produce very dramatic non-equilibrium spectral effects. For the larger beam current density, however, plasma turbulence develops which is assumed to result in anomalous resistivity. In this case, the heating is shown to be both rapid enough and large enough to produce precisely the kind of non-equilibrium effects discussed here. It is further argued that reverse current heating may, by other plasma mechanisms, raise the electron temperature even higher than shown in our illustrative calculation.

Accordingly, we have presented theoretically predicted line enhancements and decay times for a representative selection of lines prominent in the pre-flare coronal X-ray spectrum. Among these are lines which should soon be observable with, for example, the soft X-ray Polychromator planned for the Solar Maximum Mission. The spectral and time resolution of this instrument should make observation of the postulated enhancements possible.

Acknowledgments

In carrying out this research, the authors have benefited considerably from their participation in the Skylab Solar Workshop Series on Solar Flares. The workshops are sponsored by the National Aeronautics and Space Administration and the National Science Foundation and managed by the High Altitude Observatory. We would like to thank Prof. P.A. Sturrock for many helpful discussions. We acknowledge discussion with R.T. Moore. This work was supported in part by the National Aeronautics and Space Administration under grant NGL 05-020-272 and the Office of Naval Research under contract N00014-75-C-0673. One of us (P.R.S.) was supported in part by a National Science Foundation Predoctoral Fellowship.

References

Beigman, I.L., Vainshtein, L.A., Vasilyev, B.H., Zhitnik, B.N., Ivanov, V.D., Korneyev, V.V., Krutov, V.V., Mandelshtain, S.L., Tindo, I.P., and Shurygin, A.I. 1971, Kosm. Issled. 9, 123.

Brown, J.C. and Melrose, D.B. 1977, Solar Phys. 52, in press.

Chubb, T.A., Kreplin, R.W., and Friedman, H. 1966, J. Geophys. Res. 71, 3611.

Colgate, S.A., Audouze, J., and Fowler, W.A. 1976, Cal. Tech. Orange-Aid Preprint Series #458.

Correll, D.L., Ryan, N., and Bohmer, H. 1975, Phys. Fluids, 18, 1800.

Cox. J.L. and Bennett, W.H. 1970, Phys. Fluids, 13, 182.

Datlowe, D.W. 1975, in Solar Gamma-, X-, and EUV Radiation, ed. S.R. Kane (Dordrecht: Reidel), p. 191.

Davis, J., Kepple, P.C., and Strickland, D.J. 1977, J. Quant. Spect. Rad. Trans. 17, 711.

Dum, C.T. and Dupree, T.D. 1970, Phys. Fluids, 13, 2064.

Frost, K.J. 1969, Ap. J (Lett.) 158, L159.

Hammer, D.A. and Rostoker, N. 1970, Phys. Fluids, 13, 1831.

Hoyng, P., Brown, J.C., and van Beek, H.F. 1976, Solar Phys. 48, 197.

Hoyng, P., Knight, J.W., and Spicer, D. 1977, preprint.

Ionson, J.A. 1976, Phys. Letters, 58A, 105.

Kafatos, M.C. and Tucker, W.H. 1972, Ap. J. 175, 837.

Kane, S. and Anderson, K.A. 1970, Ap. J. 162, 1003.

Kato, T. 1976, Ap. J. Supplement Series, 30, 397.

Kelly, N.C., Bering, E.A., and Mozer, F.S. 1975, Phys. Fluids, 18, 1590.

Kindel, J.M. and Kennel, C.F. 1971, J. Geophys. Res. 76, 3055.

Knight, J.W. and Sturrock, P.A. 1977, Ap. J. 218, 306.

Lotz, W. 1968, Z. Physik, 216, 241.

_____. 1969, Z. Physik, 220, 466.

Mewe, R. and Schrijver, J. 1975, Astrophys. Space Sci. 38, 345.

Noyes, R.W. 1971, Ann. Rev. Astr. Ap. 9, 209.

Palmadesso, P.J., Coffey, T.P., Ossakow, S.L., and Papadopoulos, K. 1974, Geophys. Res. Letters, 1, 105.

Papadopoulos, K. 1977, Rev. Geophys. Space Phys. 15, 113.

Shapiro, P.R. and Moore, R.T. 1977, Ap. J. 217, 621.

Spicer, D.S. 1977, Solar Phys., in press.

Spitzer, L. 1962, Physics of Fully Ionized Gases (New York: Interscience).

Tucker, W.H. 1975, Radiation Processes in Astrophysics (Cambridge: Press).

Van Beek, H.F., De Feiter, L.D., and De Jager, C. 1974, in Space Research XIV, eds. M.J. Rycroft and R.D. Rosenberg (Berlin: Akademie-Verlag), p. 447.

Van Regemorter, H. 1962, Ap. J. 136, 906.

TABLE 1*†

Line Enhancement Factors (β)

Ion	Transition	λ(Å)	E_{ij}(eV)	y	α_{max}	α=10	$\alpha=\alpha_{max}$	α=100	α=300	α=1000
Mg XI	$1s^2(^1S)$ -$1s3p(^1P)$	7.85	1579.6	6.110	104	56.1	133	133	117	88.2
	$1s^2(^1S)$ -$1s2p(^1P)$	9.17	1352.2	5.231	90	28.7	58.0	58.0	50.8	37.9
Fe XVII	$2p^6(^1S)$ -$2p^54d(^1P)$	12.12	1023.1	3.958	68	11.5	19.2	18.4	15.4	11.3
	$2p^6(^1S)$ -$2p^53d(^1P)$	15.26	812.6	3.143	54	6.6	9.5	8.9	7.3	5.2
O VIII	$1s(^2S)$ -$2p(^2P)$	19.00	652.6	2.524	43	4.4	5.7	5.2	4.1	2.9
	2-4	75.90	816.78	3.160	54	6.7	9.6	9.1	7.4	5.3
O VII	$1s^2(^1S)$ -$1s2p(^1P)$	21.60	574.1	2.221	38	3.7	4.5	4.0	3.2	2.2
N VII	$1s(^2S)$ -$2p(^2P)$	24.80	500	1.943	33	3.1	3.6	3.2	2.4	1.3
S XIV	$2s(^2S)$ -$3p(^2P)$	30.43	407.5	1.576	27	2.6	2.8	2.3	1.8	1.2
C VI	$1s(^2S)$ -$2p(^2P)$	33.70	368.0	1.424	24	2.4	2.6	2.1	1.6	1.1
Si XII	$2s(^2S)$ -$3p(^2P)$	40.92	303.0	1.172	20	2.1	2.2	1.7	1.3	0.9
Fe XVI	$3s(^2S)$ -$4p(^2P)$	50.50	245.5	0.95	16	1.9	1.9	1.4	1.1	0.7
	$3d(^3D)$ -$4p(^2P)$	76.60	245.5	0.95	16	1.9	1.9	1.4	1.1	0.7

*Wavelengths and excitation energies were taken from Kato (1976).

†$T_{initial} = 3 \times 10^6$K is assumed.

TABLE 2*†

Ionization Times ($\tau_i n_e, g s \cdot cm^{-3}$)

ION	I_1(eV)/χ_1	I_2/χ_2	I_3/χ_3	ξ_1	ξ_2/ξ_3	$\alpha=10$	$\alpha=\alpha_{max}$	$\alpha=100$	$\alpha=300$	$\alpha=1000$
Mg XI	1761.79/6.815			2		38.4	21.5 (α_{max}=90)	21.6	25.2	33.7
Fe XVII	1265/4.893	1397/5.404		6	2/	4.89	3.39 (α_{max}=68)	3.51	4.24	5.79
O VIII	871.39/3.371			1		17.9	15.1 (α_{max}=54)	16.3	20.5	28.7
O VII	739.316/2.860			2		6.63	5.84 (α_{max}=38)	6.57	8.37	11.8
N VII	667.029/2.580			1		11.0	9.99 (α_{max}=33)	11.5	14.7	20.9
S XIV	706.8/2.734	3076/11.899		1	2/	11.4	9.31 (α_{max}=27)	9.89	12.2	16.8
C VI	489.98/1.895			1		6.53	6.29 (α_{max}=24)	7.68	10.1	14.5
Si XII	523.3/2.024	2310/8.936		1	2/	6.63	5.96 (α_{max}=20)	6.63	8.38	11.8
Fe XVI	490/1.895	1223/4.731	1344/5.199	1	6/2	2.68	2.33 (α_{max}=16)	2.33	2.89	4.02

*Constants are taken from Lotz (1968, 1969), where a = 4.5, b = c = 0 throughout.

†$T_{initial}$ = $3x10^6$ K is assumed.

FIGURE CAPTIONS

Figure 1. Temperature (T) as a function of integrated number density (I) from the injection point, for an energetic electron number flux of 1.414×10^{17} cm^{-2} s^{-1}. The temperature is displayed for times before the beam is injected (t = 0 s) and after the beam is injected (t = 1 s and t = 4 s).

Figure 2. Temperature (T) as a function of integrated number density (I) from the injection point, for an energetic electron number flux of 5.656×10^{17} cm^{-2} s^{-1}. The temperature is displayed for times before the beam is injected (t = 0 s) and after the beam is injected (t = .25 s and 5 = 1 s).

Figure 3. Number density (n_e) as a function of integrated number density (I) from the injection point. The model serves only to represent the gross overall structure of the solar atmosphere above an active region since the exact temperature and density structure of the atmosphere is not well established and differs from active region to active region.

Addresses

J.W. Knight
Institute for Plasma Research
Stanford University
Stanford, CA 94305

Paul R. Shapiro
Center for Astrophysics
60 Garden Street
Cambridge, MA 02138

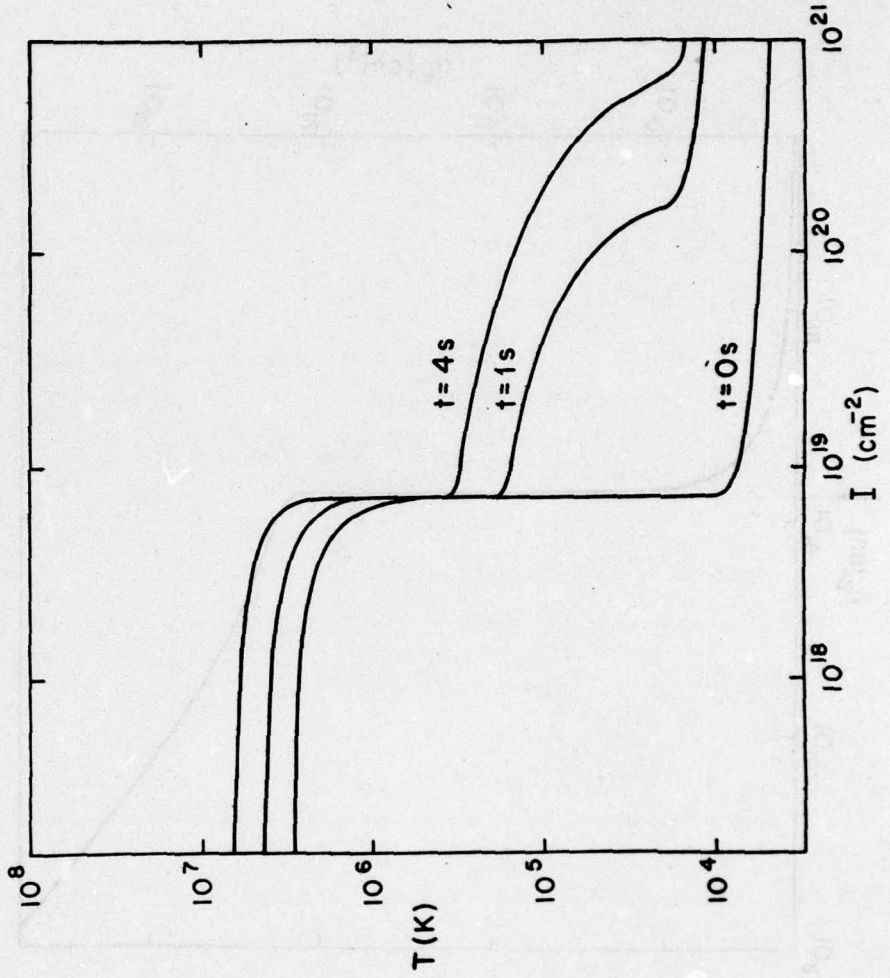

FIG. 1

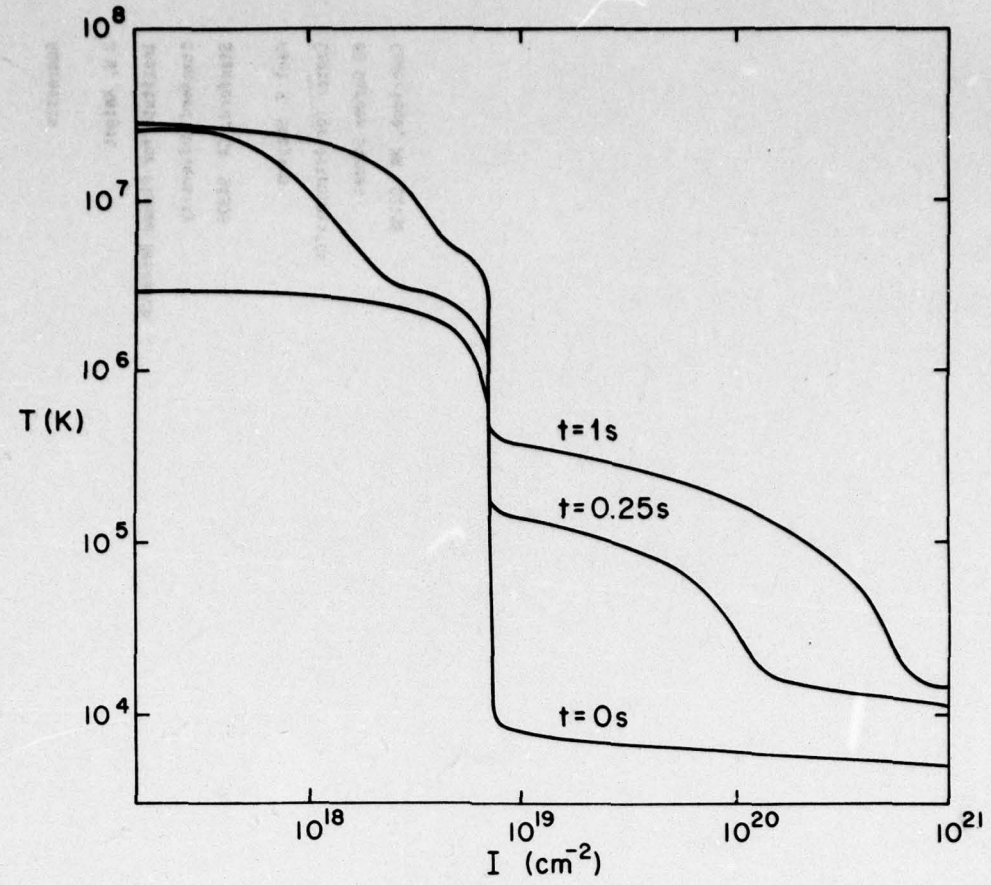
10^8
10^7
10^6
10^5
10^4
T (K)
t=1s
t=0.25s
t=0s
10^{18}
10^{19}
10^{20}
10^{21}
I (cm^{-2})

FIG. 2

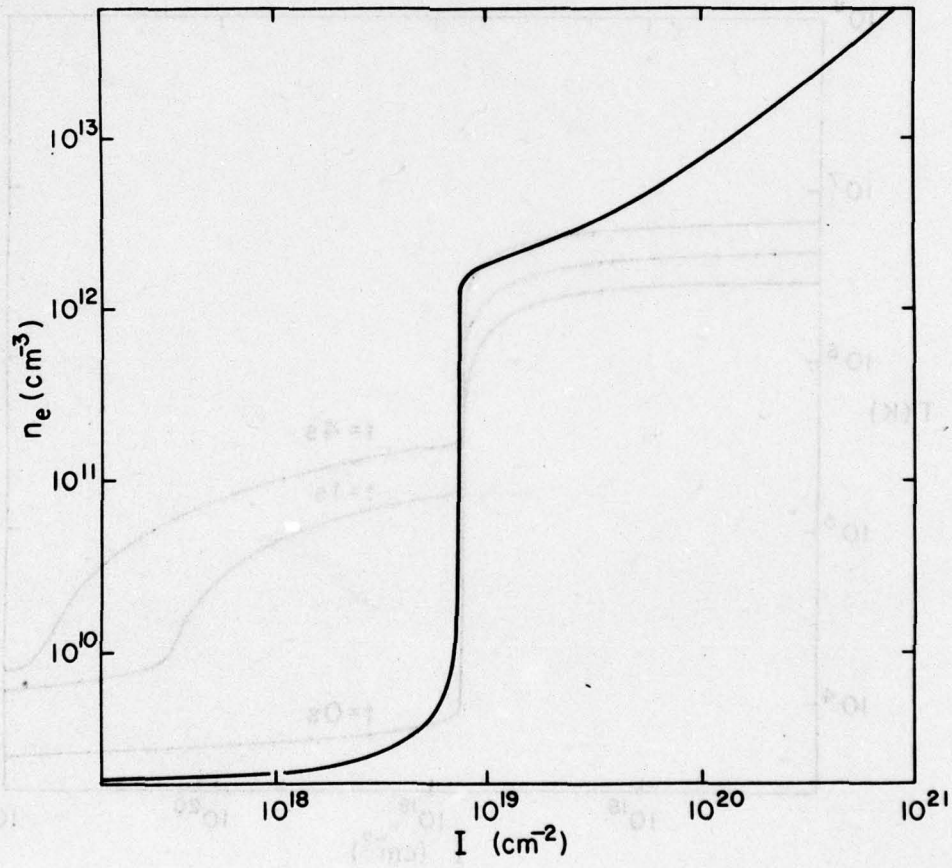
10^{13}
10^{12}
10^{11}
10^{10}
n_e (cm^{-3})
10^{18}
10^{19}
10^{20}
10^{21}
I (cm^{-2})

FIG. 3